Study on coal seam physical characteristics and influence on stimulation: A case study of coal seams in zhengzhuang block

Yanjun Lu[1], Jinxuan Han[1]*, Hua Zhang[2], Zhenping Xu[3], Zhaozhong Yang[4], Manping Yang[1], Junfeng Guo[5], Hongjian Zhu[1] and Yu Qi[1]

[1]School of Vehicle and Energy, Yanshan University, Qinhuangdao, China, [2]CNPC Bohai Drilling Engineering Company Limited, Tianjin, China, [3]Exploration and Development Research Institute of Changqing Oilfield Company, PetroChina, Xi'an, China, [4]State Key Laboratory of Oil and Gas Reservoir Geology and Exploitation, Southwest Petroleum University, Chengdu, China, [5]Shanxi CBM Exploration and Development Co., PetroChina, Jincheng, China

Coalbed Methane (CBM) is an unconventional form of natural gas which is self-generated and self-stored in coal seams. In order to realize the effective exploitation of CBM in Zhengzhuang block, microstructure, wettability, permeability, rock mechanics and in-situ stress of coal were studied in this research. It is found that high rank anthracite characterized by high vitrinite content and low inorganic mineral content, is abundant in CBM. More than 96% of inorganic minerals are clays dominated by kaolinite and illite. Various types of pores are developed on the coal. The wettability of coal differs from high to low to surface water, active water, and foam fracturing fluid; and contact angles of coal with active water and foam fracturing fluid decrease with the increase of burial depth. Gradients of fracture pressure and closure pressure in No.3 coal seam are higher than that of No.15 coal seam. The elastic modulus of coal is lower than that of sandstone. The construction curve of hydraulic fracturing shows that, when the construction flow rate and sand quantity are similar, the construction pressure of prepad in No.3 coal seam is lower than the pumping pressure of No.15 coal seam, but the propagated pressure is higher than that of No.15 coal seam. The drainage effect of No.3 coal seam with large pore volume, shallow burial depth and obvious fracture pressure is better than that of No.15 coal seam. The comprehensive understanding of coal physical properties and engineering practice in the block provide certain guiding significance to the CBM exploitation in Qinshui Basin.

KEYWORDS

coalbed methane, anthracite, pore-fissure of coal, coal physical properties, hydraulic fracturing

1 Introduction

Compared with conventional oil and gas reservoirs, CBM reservoir is characterized by low porosity, low pressure, and low permeability; the production of coalbed methane has to undergo the process of desorption, diffusion and seepage (Balan and Gumrah, 2009; Liu and Harpalani, 2013). Most coal seams must be fractured before they can be put into production (Wang et al., 2014). Through hydraulic fracturing, natural fracture system can be communicated, pollution near wellbore can be removed, and high seepage channel can be established for CBM desorption (Lu et al., 2018; Li et al., 2021). The final effect of fracturing is not only closely related to the characteristics of coal porosity and permeability, microstructure, rock mechanics, *in-situ* stress and other geological factors (Zhang et al., 2018; Xue et al., 2019; Salmachi et al., 2021; Min et al., 2022), but also affected by fracturing engineering factors (Li et al., 2020). Therefore, comprehensive reservoir geology analyzes and employ of fracturing engineering are necessary during CBM exploitation by provide developing guidance.

In the process of fracturing, fracturing fluid certainly will bring damage to coal seam, resulting in the permeability reduction and affecting the exploiting effect. Coal has high adsorption capacity for guar gum and broken organic polymer fracturing fluid (Cong et al., 2007; Gao, 2016). The damage rate of activate water to coal permeability is relatively low, and its damage to coal seam mainly comes from water sensitivity and water lock (Li et al., 2021). The contact between active water and coal matrix will produce wetting on the coal surface, and the micropore wetting will affect the desorption and seepage of gas. The decrease of contact angle indicates that the active water has good spreading effect on the coal surface, which is beneficial to the treatment of coal powder (Xu et al., 2021). The formation and propagation of fractures are controlled by surrounding rock to a certain extent. With the increase of the elastic modulus difference between coal and surrounding rock, the length of fractures formed by fracturing increases, the height decreases, and the fracture width increases. The longitudinal heterogeneity of mechanical properties of coal and surrounding rock increases the difficulty in vertical propagation of fractured fractures, which makes them easier to be confined in the coal seam and form long and wide fractures (Gao et al., 2020). In-site stress, tensile strength and cohesion are the important factors affecting the fracture propagation in coal (Teufel and Clark, 1984; Behnia et al., 2015). Whether hydraulic fracture penetrates the bedding plane depends not only on the mechanical properties difference between productive strata and interlayer, but also on the interface properties, vertical stress difference, horizontal stress difference, fracturing fluid pressure, fracture geometry and other factors (Huang and Liu, 2017). The shale—coal interface has a hindering effect on fracture propagation, and the fracture mainly extends in the horizontal direction, never crossing the rock interface (Yu et al., 2019).

In previous researches, mineral composition, macerals, mechanics and metamorphism degree of coal in Qinshui Basin have been thoroughly studied, but specific understanding of the effects of these characteristics on CBM exploitation is still a gap in the industry. In this paper, the No.3 and No.15 coal seams in Zhengzhuang block, southern Qinshui Basin are taken as examples. The influence of coal geology and engineering on CBM exploiting is comprehensively analyzed on the basis of laboratory experiments, combined with fracturing construction and on-site drainage data. The research results are expected to provide guiding significance for fracturing design.

2 Geological setting

Qinshui Basin, located in southeast Shanxi Province, is one of the areas with the most abundant carboniferous and Permian coal resources in North China. The coal seams of Taiyuan and Shanxi Formations are the targets of CBM exploration in this area. Coal measure strata are well developed and well preserved; and the tectonic structure is relatively simple and stable in Qinshui Basin. The total reserve of CBM in the basin is $3.97 \times 10^{12} m^3$, accounting for 10.8% of total geological resources of CBM in China. At present, Qinshui Basin is an area with the largest investment, the highest degree of exploration, the most active exploitation and the most significant gas recovery, so it has become one of the two CBM industrialization bases in China (Liu et al., 2019). Zhengzhuang block is in southeast Qinshui Basin (Figure 1), which has many favorable conditions for CBM exploration and exploitation, and has been an important site for CBM exploration in recent years (Li et al., 2016; Zhu et al., 2018).

3 Experimental methods

Using scanning electron microscope (SEM), X-ray diffraction (XRD), energy dispersive spectrometer (EDS), optical microscope, HARKE-SPCA contact Angle tester, permeability test, injection/pressure drop well testing and *in-situ* stress test, and triaxial mechanical test, based on micro and macro structure-composition analysis, the physical properties of CBM occurrence in No.3 and 15 coal seams in Zhengzhuang block, Qinshui Basin were analyzed: including coal structure, composition, wettability, porosity, permeability, *in-situ* stress and mechanics of coal and surrounding rock. The differences between No.3 and No.15 coal seams were discussed, and the physical characteristics of two in the block were emphatically compared and analyzed to illustrate the influence of coal physical characteristics on CBM fracturing.
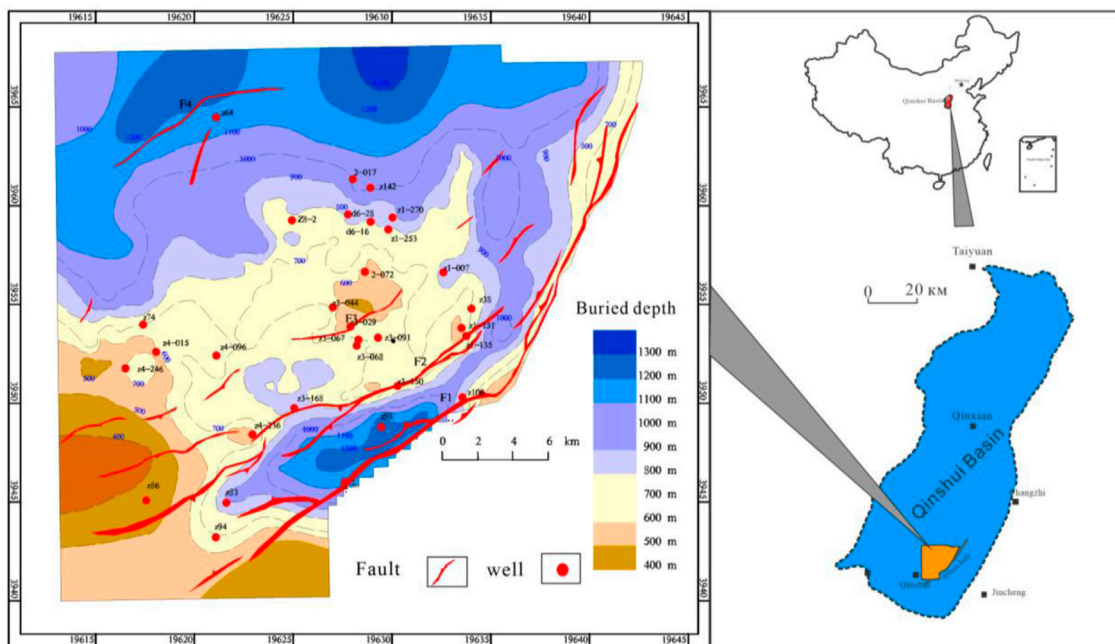
FIGURE 1
Location map of Zhengzhuang Block (modified according to Zhu and Li according to the literatures Li et al., 2016 and Zhu et al., 2018).

A Coal sample from CBM Well in No.3 coal seam-ZM74

B Coal sample from CBM Well in No.15 coal seam-ZM98

C Coal sample from roadway located in No.3 coal seam-SM1
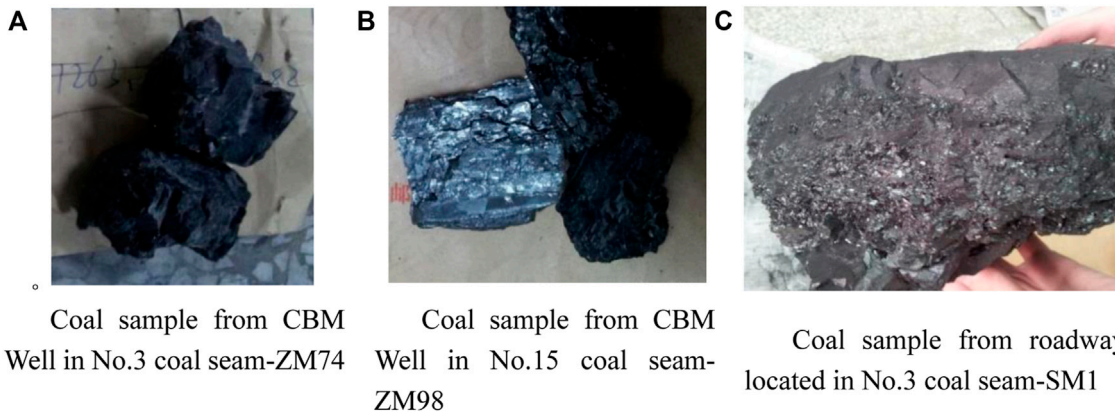
FIGURE 2
Different coal samples.

4 Sample characteristics

4.1 Apparent

Experimental core samples were collected from Zhengzhuang CBM Wells and Sihe coal mine, as shown in Figure 2. The color of coal in the area is black or gray-black, and the striation color is dark black, showing glass-strong glass luster. Endogenous fissures are not well developed; and irregular and conchoidal fractures can be observed. The natural fractures of roadway coal samples mainly exist in the form of horizontal fractures, while the natural micro-fractures of coal in CBM Wells mainly develop along the vertical direction, parallel to the wellbore direction, which is related to the coal sedimentary

FIGURE 3
SEM of coal samples.

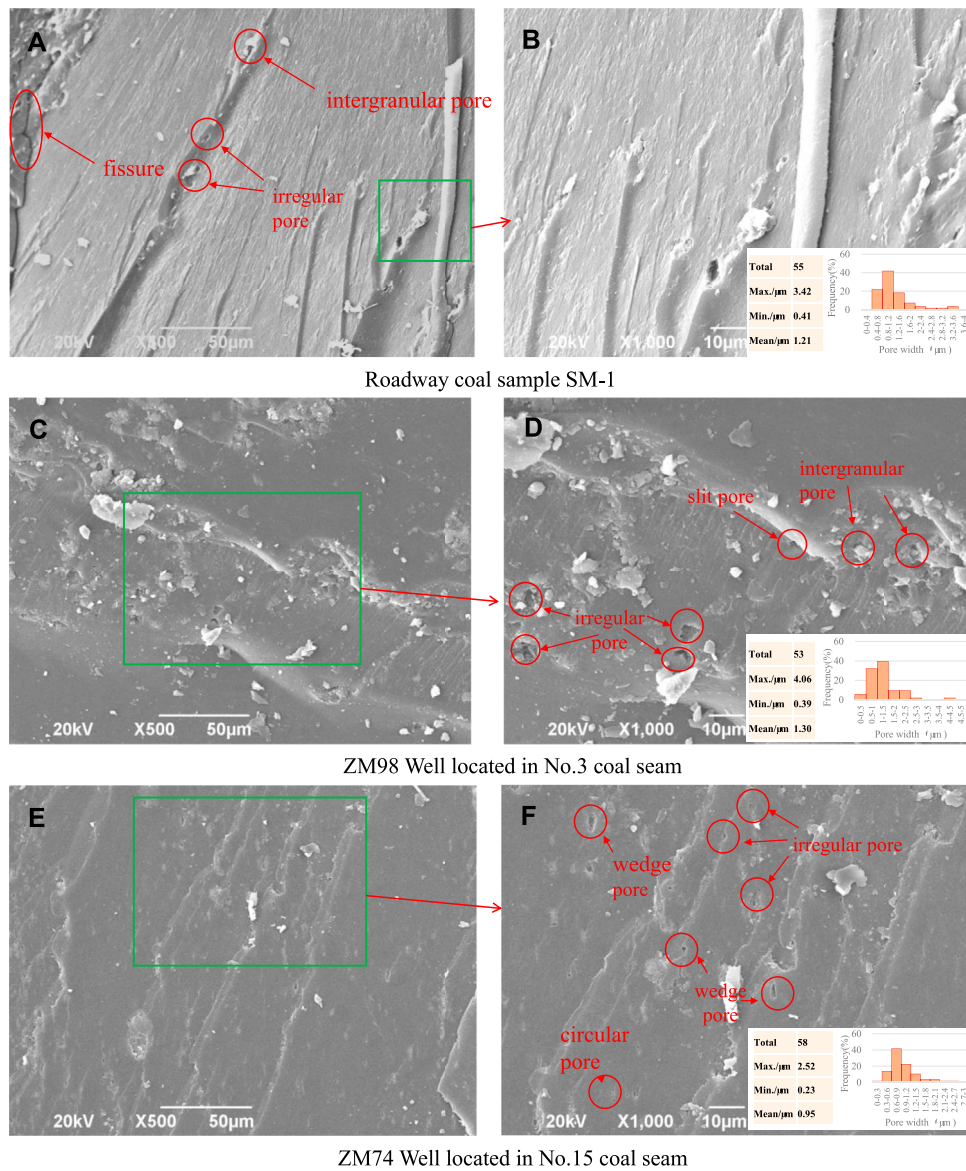environment, tectonic movement and other factors. Compared with the coal samples in the roadway, the natural fractures in CBM Wells are more developed, and the coal has obvious metallic luster.

4.2 Microstructure

The microstructure of the samples was analyzed by SEM (Figure 3). It can be observed that there are different forms of pores and fissures on the coal surface, mainly pores by SEM. Most of the pores are uneven and partially filled or inlaid with clay.

Types of pores include wedge, circular, irregular and slit. Point counting and measurements of pores in SEM images were done using Nano Measurer 1.2 software, and maximum pore size, minimum pore size, average pore size and pore size distribution in coal samples were obtained (Figure 3). The results show that under the same magnification (×1,000 times), the average pore size of roadway coal sample (No.3 coal) is 1.21 μm, the average pore size of No.3 coal seam is 1.30 μm, and the average pore size of No. 15 coal seam is 0.95 μm. It can be seen that the average pore size of No.3 coal seam is larger than that of No. 15 coal seam. According to Hodot's classification of pore size, coal pore can be divided into micropore (<10 nm), transition pore (10–100 nm),

FIGURE 4
Pore characteristics of No. 3 and No. 15 coal seams (Hu et al., 2015).
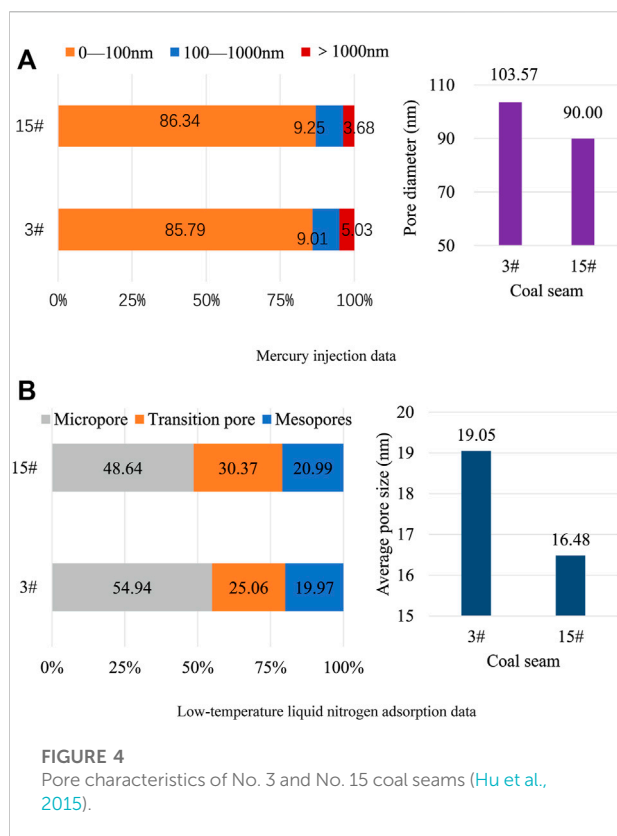
mespore (100–1000 nm) and macropore (>1000 nm) (Hodot, 1966). Mercury injection can be used to study the distribution of transition pores, mesopores and macropores. Mercury injection data show that the pore size of No. 3 and No. 15 coal seams is mainly concentrated in 0–100 nm (as shown in Figure 4A). The proportion of pore size with 0–100 nm in No. 15 coal seam is higher than that in No. 3 coal seam, while the proportion of pore size over 1000 nm is lower than that in No. 3 coal seam. The mean pore diameter of No. 3 coal seam (103.57 nm) is larger than that of No. 15 coal seam (90 nm). This is consistent with the SEM results that No. 3 coal seam has more large pores, while No. 15 coal seam has more small pores. Low-temperature liquid nitrogen adsorption can be used to analyze the distribution of micropores, transition pores and mesopores. The adsorption data show that the average pore size of No. 15 coal seam is lower than that of No. 3 coal seam, but the proportion of transition pores and mesopores in No. 15 coal seam is slightly higher than that in No. 3 coal seam, indicating that the pore diameter of No. 15 coal seam is generally smaller in the same pore size segment (Figure 4B) (Hu et al., 2015).

In summary, the data of SEM, mercury injection and low-temperature liquid nitrogen adsorption show that the proportion of large pores, pore throat radius and average pore size of No. 3 coal seam are larger than those of No. 15 coal seam, and the

pore structure is generally better, which is conducive to CBM exploitation.

4.3 Maceral and mineral analysis

Macerals are the smallest organic particles of coal which can be observed under microscope. Because they are composed of vegetation from different regions, they have different optical properties and chemical composition. The test results show that the vitrinite reflectance (R_o) of coal samples is 3.72–3.93%. The maceral is composed of vitrinite and inertinite without exinite. Mineral content is relatively low, accounting for 1–3.1% (Table 1). The vitrinite reflectance and mineral content of coal samples from coal mines and Wells are close to each other, indicating that the coal in this area all belong to high rank anthracite.

The organic residues of plants constitute the main part of coal, but inorganic substances (minerals) are involved in the whole process of converting vegetation into coal without exception. It is not only a part of coal, but also affects the conversion process of organic materials. The inorganic components in coal are mainly clay minerals, which are the main source of ash content. The distribution of carbonate minerals in coal is second only to clay minerals, including calcite, siderite and dolomite, etc. The most common sulfide mineral is pyrite, which is mostly found in shallow sea or coastal coal. Silica is mainly from quartz, mostly in the form of a single particle or larger block. By XRD experiments, the inorganic minerals of coal in Zhengzhuang block are mainly clay, quartz, potash feldspar, calcite and dolomite, of which clay accounts for 95%–98% (Table 1).

The mineral composition of the samples was analyzed by EDS. The white particles distributed on the coal surface are clay minerals, mainly kaolinite and illite. Kaolinite is a relatively stable non-swelling clay mineral which is not easy to be hydrated, it discontinuously distributes in the pore wall or fills in the pore space (Figure 5A), narrowing the pore. However, due to poor mechanical resistance of kaolinite, it is easy to cause cleavage cracking and disperse into scaly particles under external force, which damages the permeability of CBM reservoir. Illite is also a kind of non-expanding clay mineral, mostly dispersed in pores in a thin film shape, which is easily broken into discrete particles migrated with the fluid under the impact of high-speed fluid (Figure 5B), blocking the pore throat channel and affecting the diffusion and seepage of methane in coal seam.

The existence of clay minerals will have adverse effects on fracturing and drainage gas recovery of coal seam. On one side, the permeability of reservoir decreases and the fluid flow is affected due to the blockage of pores and fissures in coal. On the other side, it can weaken the mutual support strength of coal particles, lead to the production of coal powder, and affect the fracture conductivity and drainage effect after fracturing.

TABLE 1 Component analysis of coal samples.

Sample	Depth (m)	Maceral content (%)			Mineral content (%)	Mineral type and proportion (%)					Vitrinite reflectance R_o (%)
		Vitrinite	Inertinite	Exinite		Clay	Quartz	Potash feldspar	Calcite	Dolomite	
3#SM1	300–305	81.6	16.8	-	1.6	96	0	1	0	3	3.93
15#ZM74	958–959	84.3	14.2	-	1.5	95	1	2	0	2	3.85
3#ZM94	687–692	85.6	11.3	-	3.1	97	2	1	1	0	3.89
3#ZM98	1,232–1,233	77.8	21.2	-	1	98	1	1	0	0	3.72

FIGURE 5
EDS of coal.
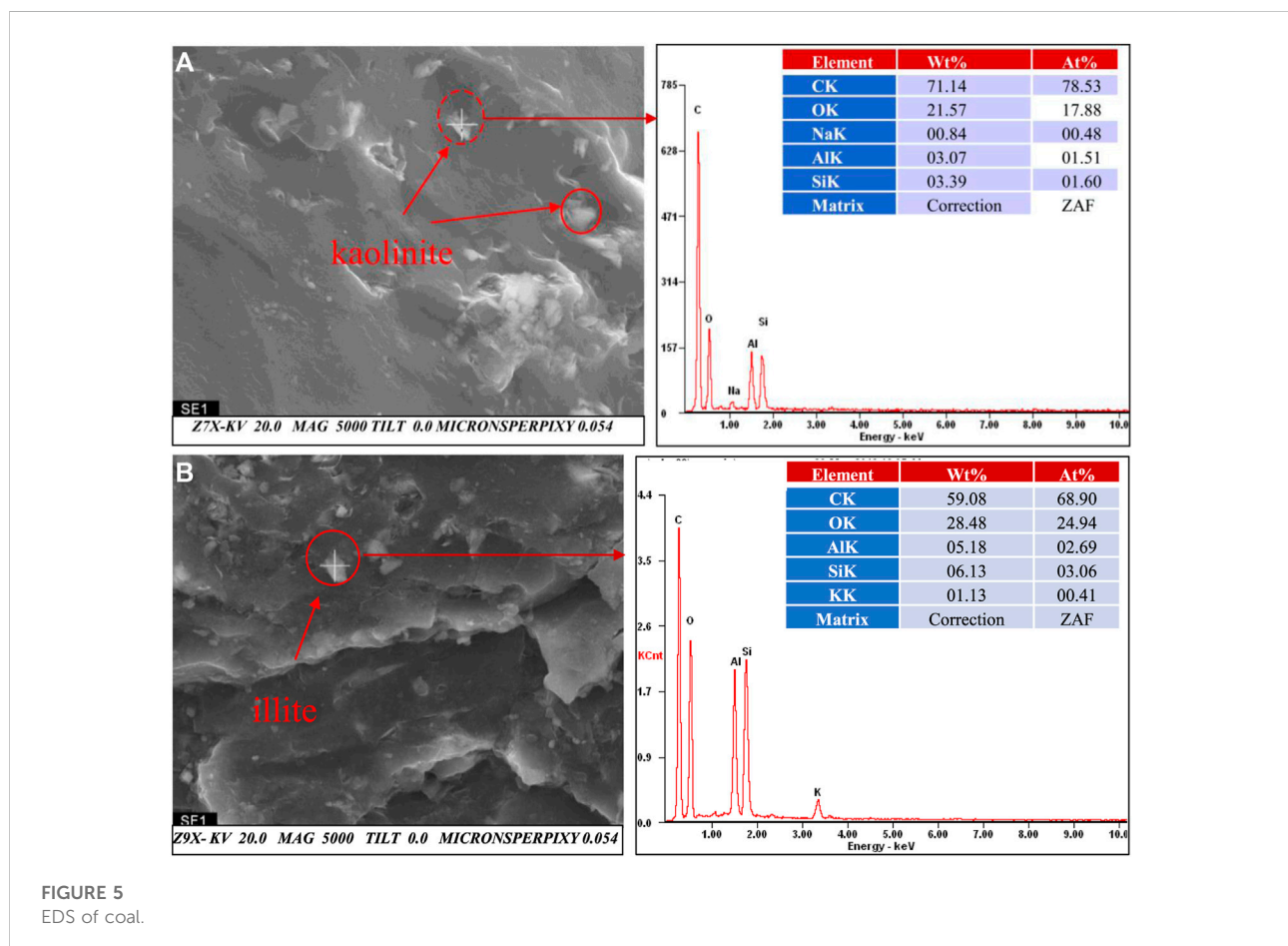
5 Discussion

5.1 Surface wettability

Wettability of coal can be affected by coal rank, chemical composition, oxygen-containing functional groups, composition and porosity (Li and Li, 2016). In the formation of high rank coal, the side chains and functional groups of coal fall off continuously, resulting in the increasing number of aromatic rings, closer arrangement of aromatic lamella, reduced spacing, decreased porosity, weakened hydrophilicity of coal and enhanced adsorption gas.

In this research, the wettability of coal was studied by HARKE-SPCA contact Angle tester, and the study liquids were surface water, active water fracturing fluid and foam fracturing fluid. The results are shown in Figure 6. By experiments, wetting angles of the three coal samples to surface water are 44°, 57° and 29° respectively, indicating
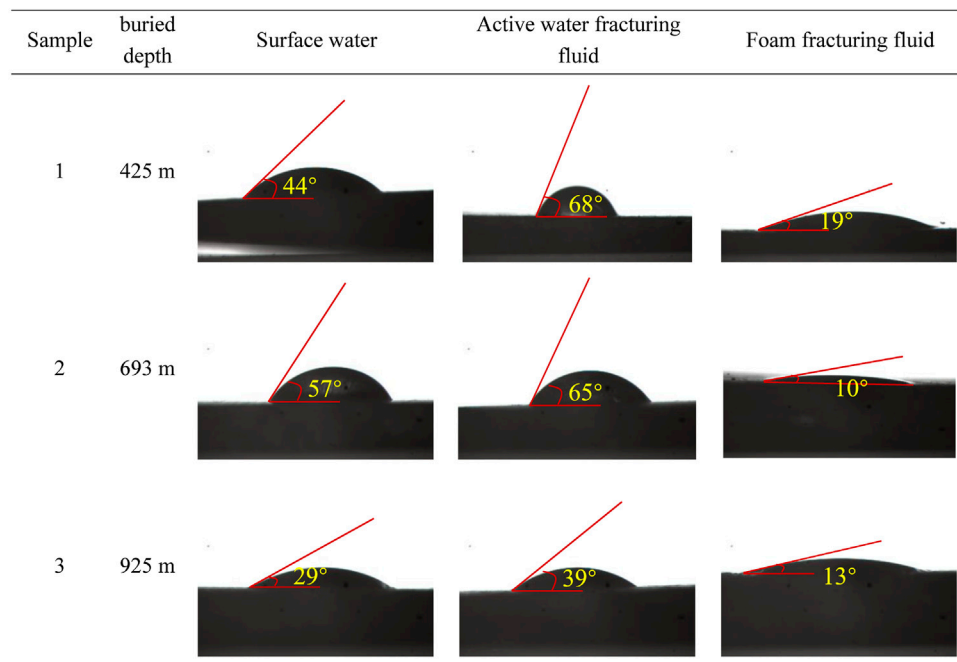
FIGURE 6
Wetting angle measurement results.

hydrophilicity. by adding surfactants into surface water, the contact angles become larger, respectively 68°, 65° and 39°, and the wettability becomes worse. However, after adding foaming agent into surface water, the contact angles between coal and foam fracturing fluid are 19°, 16° and 13°, respectively, and the wettability becomes better. It can be seen that coal heterogeneity results in differences in wettability of coal samples to the same liquid, and with the increase of sample depth, the contact angle with active water and foam fracturing fluid presents a trend of decrease, that is, increases in hydrophilicity.

The influence of wettability on CBM fracturing is multifaceted. When the contact angle is large, the coal powder has strong hydrophobicity and poor dispersion in water, make it easy to accumulate at the end of fractures to form blockage. When the contact angle is small, the liquid has good wettability on the coal surface, and the coal powder is discharged with the flow back fluid, which reduces the damage to the reservoir. In addition, at a low contact angle, water molecules will form adsorption water film on the surface of pores and fissures, narrowing the channel of methane diffusion and seepage, thus affecting the production of CBM (Li et al., 2016). Therefore, the system of fracturing fluid needs to be selected according to the actual situation. For the Well with serious pulverized coal, the liquid with good wettability can be used as far as possible, and conversely, the hydrophobic liquid system can be used.

5.2 Permeability

The permeability test of coal samples in roadway shows that the permeability is generally very low, and the value ranges from 0.003mD to 0.068mD (Table 2). Under similar external conditions, different permeability reflects the difference of fissure and pore distribution. According to the data, the permeability of CBM Wells in the study area is 0.015–0.29mD, and the porosity is 3.33–6.53% (Table 2) (Zhang, 2018).

Although the pores of coal matrix have certain permeability, it is far less than the cleat permeability of coal. Fluid only flows in the cleats, so the permeability reflected in the test is the comprehensive permeability dominated by cleat permeability. The coal of Zhengzhuang block belongs to ultra-low permeability and low porosity reservoir. Permeability statistics show that permeability and porosity of coal seam are affected by depth to a certain extent. As is shown in Figure 7, the inflection point of porosity and permeability appears near 800 m and 720 m depth respectively, and then decreases with the increase of depth. Significant changes in gas content and permeability can be observed with depth. This change is related to coal rank, sealing ability of overlying strata, measurement method, thermal effect of magmatic intrusion, geological structure and stress state (Salmachi et al., 2021).

TABLE 2 Permeability and porosity of coal samples in Zhengzhuang block.

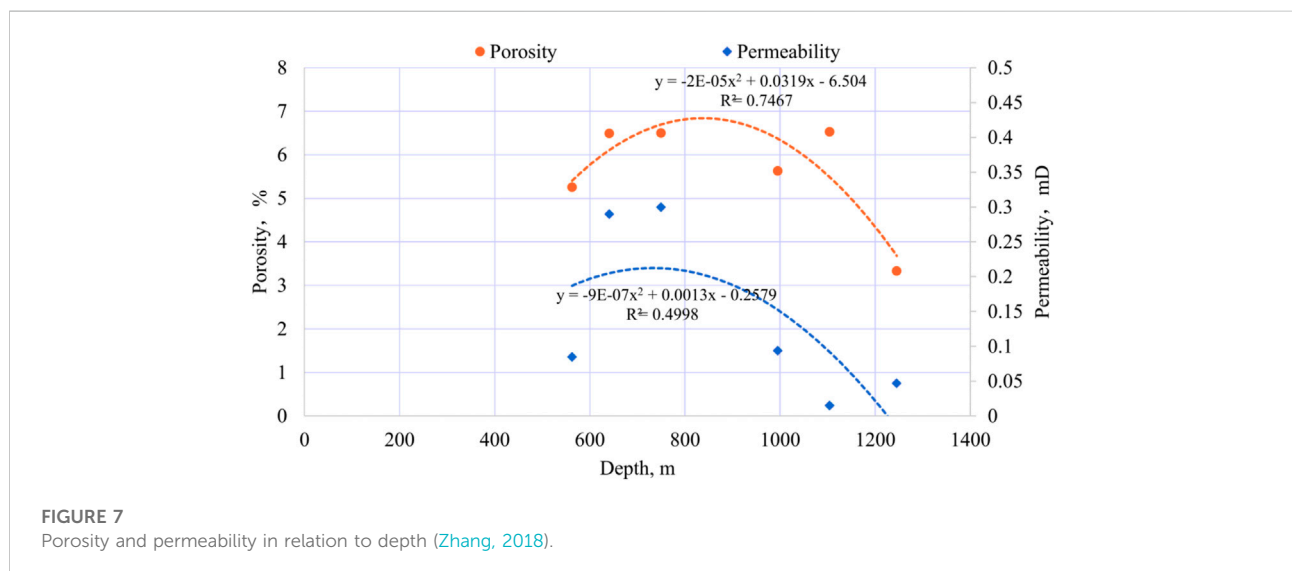| Sample/Well	Depth (m)	Permeability (mD)	Porosity (%)
Coal samples in Sihe coal mine			
1	/	0.068	/
2	/	0.018	/
3	/	0.010	/
4	/	0.003	/
5	/	0.043	/
Coal samples from CBM Wells (Zhang, 2018)			
ZS19	562.85	0.085	5.26
ZS27	749.70	0.300	6.5
ZS30	641.06	0.290	6.49
ZS39	995.29	0.094	5.63
ZS64	1,245.26	0.047	3.33
ZS102	1,104.30	0.015	6.53

FIGURE 7
Porosity and permeability in relation to depth (Zhang, 2018).

TABLE 3 Injection/pressure drop well testing and *in-situ* stress test of Well—Z38.

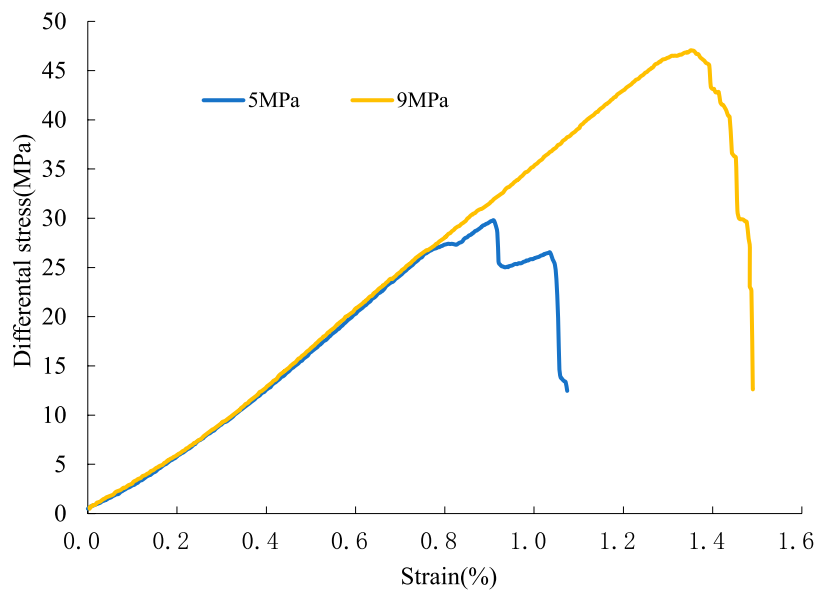| Coal seam	Thickness (m)	Middle depth (m)	Geothermal gradient (°C/100 m)	Reservoir pressure coefficient	Breakdown pressure (MPa)	Permeability (mD)	Closure pressure (MPa/100 m)
3#	5.30	662.4	4.31	1.05	19.59	0.02	2.85
15#	2.27	753.0	4.51	9.22	14.17	3.13	1.61

FIGURE 8
Stress-strain curves of coal samples at different confining pressures.

TABLE 4 Mechanical parameters obtained at different confining pressures.

Coal seam	Sample	Confining pressure (MPa)	Poisson's ratio	Elastic modulus (MPa)	Maximum differential stress (MPa)	Cohesion (MPa)	Internal friction angle (°)
Coal seam							
3#	A901	5	0.285	3,114.9	29.8	1.77	43.16
	A903	9	0.178	3,443.8	47.1		
Roof and floor							
3#	3-46-1	11.9	0.198	13013.2	72.3	6.61	40.35
	3-46-2	7	0.259	13451.3	54.3		
15#	15-100-1	14.7	0.207	9,997.3	58.3	19.59	13.29
	15-100-2	8	0.146	9,712.7	54.3		

5.3 *In situ* stress characteristic of coalbed methane reservoir

The intensity and direction of *in-situ* stress not only dominate the morphology of hydraulic fractures, but also have great influence on reservoir permeability during drainage. Injection/pressure drop well testing and *in-situ* stress test were carried out on the No.3 and No.15 coal seams of Well - Z38

(Table 3) to obtain reservoir parameters (permeability, reservoir pressure and temperature, breakdown pressure and closure pressure, etc.), providing reliable parameter basis for production potential evaluation and exploitation test of surrounding areas.

According to Table 3, compared with No.15 coal seam, No.3 coal seam has higher reservoir pressure and closure pressure gradient, but the geothermal gradient and

TABLE 5 Fracturing geology and operation parameters.

Number	M1	M2
Depth	840.6–846.5	1,095.45–1,099.3 m
Exploited coal seam	No.3	No.15
Thickness (m)	5.9	3.85
Gas content (m³/t)	20.95	22.19
Fracturing fluid volume (m³)	813.78	726.11
Fracturing fluid type	Clear water+0.5%KCl +0.1% discharge aiding agent	Clear water+0.5%KCl +0.1% discharge aiding agent
Proppant type	Quartz sand	Quartz sand
Proppant volume (m³)	40.03	40.00
Proppant mesh (mm)	0.425–0.85	0.425–0.85
	0.85–1.18	0.85–1.18

permeability is lower than No.15 coal seam. It can be seen that the higher the minimum horizontal principal stress (approximately equal to the closure pressure) is, the permeability is lower, and the breakdown pressure is positively correlated to the closure pressure.

The lower sealing pressure gradient, breakdown pressure and higher permeability of No.15 coal seam provides more advantages in fracturing operation and gas production compared with No.3 coal seam.

5.4 Mechanical characteristics of coal

1) Coal seam

In order to determine the mechanical parameters of coal, triaxial mechanical tests were carried out on samples from No.3 coal seam. Differential stress-strain curves at different confining pressures are shown in Figure 8. When the confining pressure rises from 5 MPa to 9MPa, the slope of the differential stress-strain curve increases and the pressure at the fracture point increases.

In the triaxial experiment, fractures in coal determine the uniaxial compressive strength, which is very sensitive to the heterogeneity and fracture distribution of samples, resulting in uncertainty in the experiment. In order to reduce the occurrence of the uncertainty, the triaxial compressive strength test was carried out at lower confining pressure. The results show that the stress-strain curve has a concave shape in general, which is caused by the closure phenomenon of cleats in coal at compressive stress. The degree of concave in the initial time indicates the closure stiffness of gaping fracture under certain conditions.

Young's elastic modulus, Poisson's ratio, internal friction angle and other parameters obtained from rock mechanics experiments are shown in Table 4. The density of coal is much lower than that of conventional sandstone and

carbonate, averaging 1.440 g/cm³, Poisson's ratio averaging 0.223, and elastic modulus averaging 3,251.05 MPa.

2) Roof and floor

The roof and floor of Zhengzhuang block are mostly tight sandstone and shale. According to the triaxial mechanical experiments of the roof and floor, the average Poisson's ratio is 0.20, the average elastic modulus is 11.74 GPa (Table 4), the average cohesion is 9.95MPa, and the average internal friction angle is 26.63°, indicating that the roof and floor have good sealing ability, reflecting the low or medium development of tectonic fissures in this area. The gas content of coal reservoir is generally higher in the stable tectonic zone, far from fold axis and fault zone. In addition, the mechanical strength of reservoir roof and floor is higher than that of coal, which leads to increased resistance of formed hydraulic fracture when it expands in surrounding rock, and local distortion occurs in the path of hydraulic fracture propagation, but the fracture can still maintain a certain opening, providing a channel for fluid migration.

The permeability of No.15 coal seam is higher than that of No.3 coal seam, and the sealing pressure gradient and breakdown pressure are lower, which has advantages in fracturing operation and gas production.

6 Effect analysis of field application

6.1 Hydraulic fracturing

In order to increase CBM production, some stimulation measures need to be taken, among which hydraulic fracturing is the key technology of CBM stimulation in this area (Cao et al., 2020). Well M1 and Well M2 are two CBM Wells exploited in No.3 coal seam and No.15 coal seam respectively, both are completed by casing perforation. Preliminary laboratory experiments show that the clay content in Zhengzhuang block
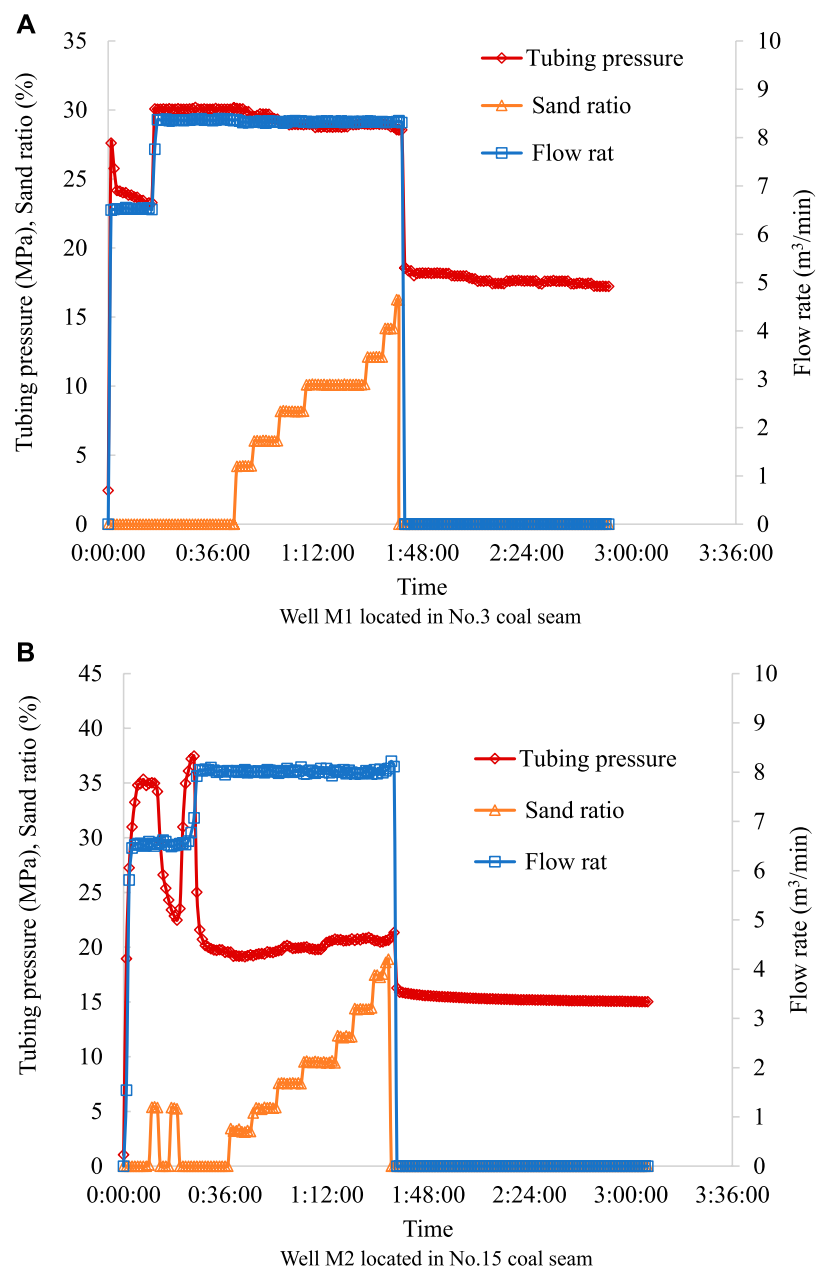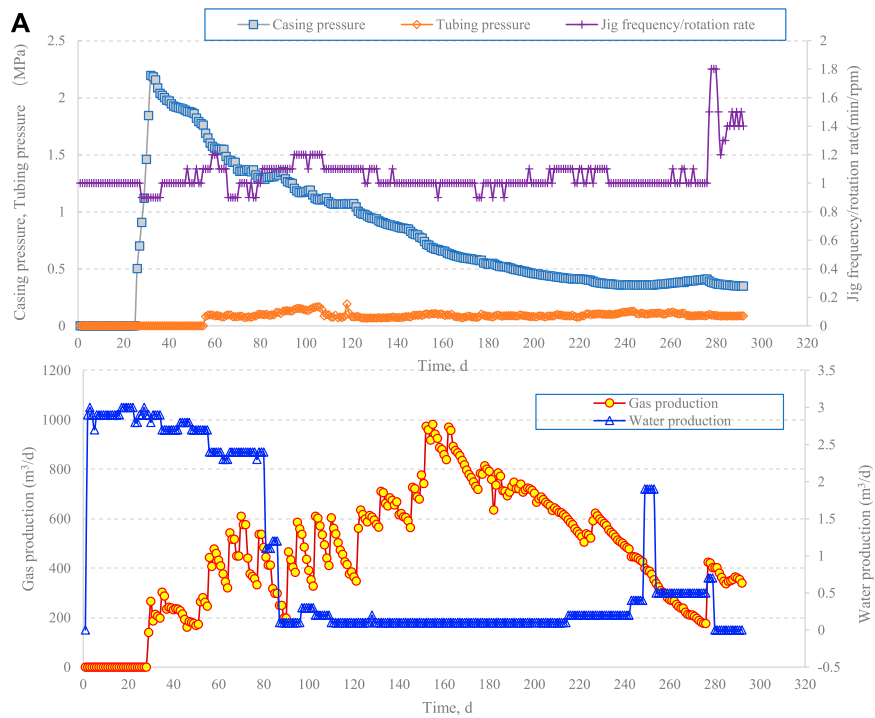
FIGURE 9
Fracturing curves of the Wells.

is low, so clear water or active water with a large contact angle with coal can be used for fracturing, and quartz sand can be selected for construction according to the closure pressure of the block. The geological parameters and fracturing data of the two Wells are shown in Table 5.

Well M2 is located at a depth of 1,095.45–1,099.3 m. The depth and gas content of Well M2 is larger than that of Well M1, but thinner than that of Well M1. The actual sand addition was equal in both, but the total fluid volume in Well M1 was slightly

higher than that in Well M2. Fracturing operations were completed on both, as shown in Figure 9.

As can be seen from the fracturing construction curve, the breakdown pressure (27.59 MPa) of Well M1 is more obvious than that of Well M2. The flow rate of prepad fluid is 6.5–8.39 m³/min with an average of 7.75 m³/min. As the flow rate increases, the construction pressure increases significantly, which is caused by the increased friction of the string and fracture at high flow rate, so that the maximum injection pressure has reached 30.17 MPa. The

Well M1 located in No.3 coal seam
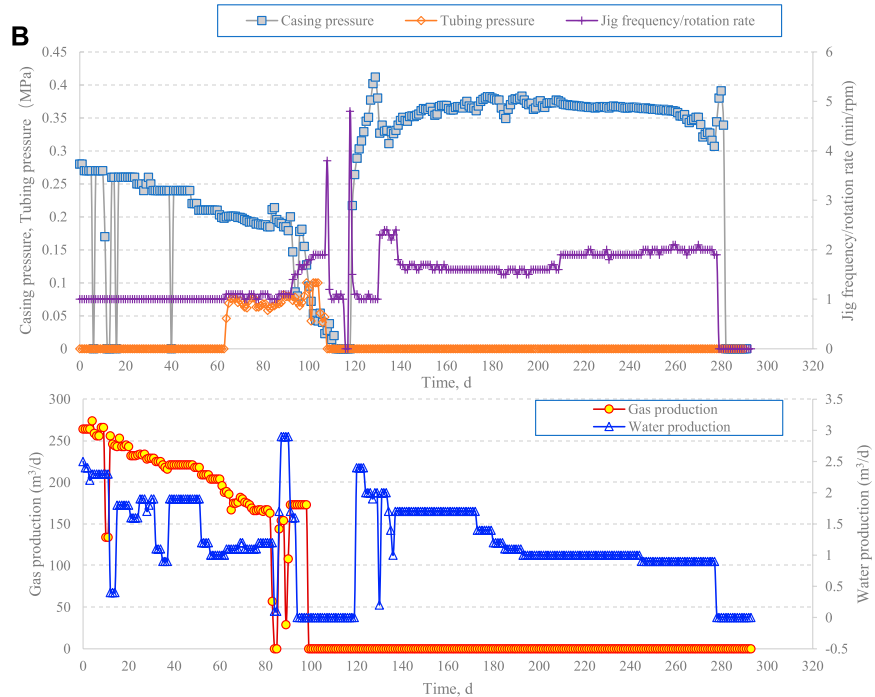
Well M2 located in No.15 coal seam

FIGURE 10
Production curves of the Wells.

average flow rate of carrying fluid is 8.32 m³/min. With fracture propagation and proppant addition, fluid column pressure of wellbore increases, and fracture propagation pressure shows a downward trend, but it is higher than that of Well M2. The pressure of pump stopping is 18.56MPa, and the pressure after pressure fall-off test is 16.8 MPa. The actual injection volume of Well M1 is 813.78 m³, quartz sand addition is 40.03 m³ (0.425–0.85 mm quartz sand—20 m³, 0.85–1.18 mm quartz sand - 20.03 m³), and the average sand ratio is 8.45%.

In the construction stage of Well M2, the flow rate of prepad fluid is 6.5–8.0 m³/min, the average flow rate is 6.88 m³/min, the highest construction pressure is 37.47MPa, and the total injection volume of prepad fluid is 250.8 m³. In the prepad stage, the slug is injected twice with 5% sand ratio. The particle size of quartz sand in the slug is 0.425–0.85 mm, and 2.0 m³ is injected in total. In the sand-carrying stage, the average flow rate is 8.01 m³/min, and 461.9 m³ of carrying fluid is injected accumulatively, of which 38 m³ of sand is injected, and the average sand ratio is 8.23%.According to the results of *in-situ* stress test, the closure pressure of No.15 coal seam is lower than that of No.3 coal seam, so the average fracture propagation pressure of Well M2 is lower than that of Well D6-18 located in No.3. The pressure fall-off test is carried out after the fracturing construction, and the pressure drops from 16.5 MPa to 15.0MPa, which is close to the formation pressure. It is further verified that the pressure coefficient of No.15 coal seam is lower than that of No.3 coal seam.

6.2 Drainage gas recovery after fracturing

Gas drainage of pumping well is performed in Wells M1 and M2 after hydraulic fracturing, with a total of 292 days. The drainage data are shown in Figure 10A and Figure 10B. The results show that the average daily gas and water production of Well M1 are 458.51 m³ and 0.91 m³ respectively, and the gas production is significantly higher than that of Well M2. As the drainage reduces the pressure, the pressure relief area of coal seam increases, coal seam water is discharged from the wellbore, and the effective desorption area gradually expands. The produce of gas begins when the critical desorption pressure is reached, and the gas production increases slowly and steadily with the growth of exploiting time. The peak of gas production occurred in Well M1 about 160 days after drainage. With the continuous decrease of casing pressure, the water production is almost zero, and the gas production also shows a decreasing trend. The average gas production of Well M2 is 67.56 m³/d, and the average water production is 1.18 m³/min. In the early stage of drainage, the gas production reaches the highest point, but with the progress of drainage, the gas production declines. In about 100 days, production stops, and the corresponding casing pressure also reaches its lowest value. In the later stage, the water production gradually decreases from 2 m³/d to 0 m³/d. Gas production is mainly affected by reservoir reserves and stimulation. Due to the high number of micropores in No.15 coal seam, the gas content of No.15 coal seam is larger

than that of No.3 coal seam, but the smaller the pores are, the greater the adsorption potential energy of methane is, and the more difficult it is to desorb. Therefore, the actual gas production of No.15 coal seam is lower than that of No.3 coal seam. In addition, the thickness of No.15 coal seam is thin, and the strength of roof and floor rock is weak, which is easier to crush through adjacent aquifers, leading to high water production in the process of drainage.

According to the results of drainage gas recovery, the gas production of No.3 coal seam is better than that of No.15 coal seam, but it is not enough to meet the requirements of industrial exploiting. It is considered that the main causes of deficiency are from two aspects: First, the coal seam in this area has a large burial depth, and the compaction of gas-bearing reservoir under pressure is characterized by low porosity and low permeability; Secondly, the coal elastic modulus is low, and the fractures generated by fracturing are relatively short, and the fractures have the possibility of closure at high stress after a period of drainage. Beyond that, the thickness of the coal seam is relatively thin, and the coal seam may be crushed at high pressure, resulting in fractures connecting the upper and lower aquifers, causing serious water invasion, affecting the CBM desorption.

7 Conclusion

Zhengzhuang block of Qinshui Basin is the main area of CBM production in China in the future. Through the comprehensive study on the microstructure, composition, porosity, permeability and mechanical characteristics of coal in the study area, the following conclusions are drawn:

1) No.3 coal seam in Zhengzhuang block belongs to high rank anthracite, with an average vitrinite reflectance of 3.82%, which belongs to the same type of coal from the roadway in this area. There are circular, wedge-shaped and irregular pores and micro-fissures in coal, and the pores are the main space for CBM occurrence. Compared with No.3 coal seam, No.15 coal seam has smaller aperture, more pores per unit area and higher gas content.

2) Causing by differences in components, the surface of coal has different wettability to different liquids, and weak hydrophilicity is expected because it facilitates the flowback of fracturing fluids. In Zhengzhuang block, in order to control the cost of fracturing fluid and reduce the damage of coal seam effectively, clear water is commonly used during coal seam fracturing. Quartz sand is selected as proppant based on the burial depth and closure pressure of the study area. Mechanical experiments show that the Poisson's ratio of coal is 0.175–0.285, with an average of 0.209; and the elastic modulus is 2,593.5–3,443.8MPa, with an average of 3,147.3 MPa. Low Young's modulus indicates that wide artificial fractures are easily formed in coal seam.

3) The coal in Zhengzhuang block has the characteristics of low porosity and low permeability, so stimulation technology has

to be put into production. According to the field fracturing construction curve, the fracture initiation pressure is not obvious, the construction pressure is greatly affected by the flow rate, and the fracture propagation pressure is significantly affected by the *in-situ* stress. The drainage data after fracturing show that the production of No.3 and No.15 coal seams does not exceed 1000 m^3. From the perspective of industrial production, the exploitation of the two Wells is not successful, mainly because of the low permeability of CBM reservoir, and the effective of communication range of artificial fractures, which is not conducive to the desorption and seepage of CBM. For Wells with low production from initial fracturing, refracturing technology is suggested in later stage of production to increase the stimulated reservoir volume and desorption area for further enhancing gas recovery.

Data availability statement

The datasets presented in this study can be found in online repositories. The names of the repository/repositories and accession number(s) can be found in the article/supplementary material.

Author contributions

YL—Writing the article; JH—Reviewing the article; HuZ and ZX—Data analysis; ZY—Project management; MY—Supervisor; HoZ—Methodology; YQ—Resources. All authors contributed to the article and approved the submitted version.

Conflict of interest

HuZ was employed by CNPC Bohai Drilling Engineering Company Limited. ZX was employed by Exploration and Development Research Institute of Changqing Oilfield Company, PetroChina. JG was employed by Shanxi CBM Exploration and Development Co., PetroChina.

The remaining authors declare that the research was conducted in the absence of any commercial or financial relationships that could be construed as a potential conflict of interest.

Publisher's note

All claims expressed in this article are solely those of the authors and do not necessarily represent those of their affiliated organizations, or those of the publisher, the editors and the reviewers. Any product that may be evaluated in this article, or claim that may be made by its manufacturer, is not guaranteed or endorsed by the publisher.

References

Balan, H. O., and Gumrah, F. (2009). Assessment of shrinkage-swelling influences in coal seams using rank-dependent physical coal properties. *Int. J. Coal Geol.* 77, 203–213. doi:10.1016/j.coal.2008.09.014

Behnia, M., Goshtasbi, K., Marji, M. F., and Golshani, A. (2015). Numerical simulation of interaction between hydraulic and natural fractures in discontinuous media. *Acta Geotech.* 10, 533–546. doi:10.1007/s11440-014-0332-1

Cao, L., Yao, Y., Cui, C., and Sun, Q. (2020). Characteristics of *in-situ* stress and its controls on coalbed methane development in the southeastern Qinshui Basin, North China. *Energy Geosci.* 1, 69–80. doi:10.1016/j.engeos.2020.05.003

Cong, L. Z., Chen, J. F., Li, Z. P., and Zhang, S. A. (2007). Adsorption features of fracturing fluid by coal substrate during the fracturing process in coalbed methane well. *Coal Geol. Explor.* 35, 27–30.

Gao, X. D., Wang, Y. B., Ni, X. M., Tao, C. Q., and Zhao, S. H. (2020). Mechanical properties of deep coal and rock in Linxing area and its influences on fracturing of deep coal reservoir. *J. China Coal Soc.* 45, 912–921.

Gao, X. (2016). Evaluation of fracturing-fluid damage for permeability in coal seam, Liulin Area, Ordos Basin. *Nat. Gas. Explor. Dev.* 39, 53–56.

Hodot, B. B. (1996). *Outburst of coal and coalbed gas (Chinese translation)*. Beijing, China: China Industry Press.

Hu, Z. Z., Huang, W. H., Lu, X. X., Xu, Q. L., Zhang, Q., and Chen, Y. P. (2015). Correlation analysis on pore characteristics of No. 3 and No. 15 coal seams in southern Qinshui Basin. *Coal Sci. Tech.* 43, 173–178.

Huang, B., and Liu, J. (2017). Experimental investigation of the effect of bedding planes on hydraulic fracturing under true triaxial stress. *Rock Mech. Rock Eng.* 50, 2627–2643. doi:10.1007/s00603-017-1261-8

Li, C., Liu, D., Cai, Y., and Yao, Y. (2016). Fracture permeability evaluation of a coal reservoir using geophysical logging: A case study in the Zhengzhuang area, southern Qinshui Basin. *Energy Explor. Exploitation* 34, 378–399. doi:10.1177/0144598716631664

Li, J. Y., and Li, K. Q. (2016). Influence factors of coal surface wettability. *J. China Coal Soc.* 41, 448–453.

Li, M., Chen, L., Bao, W. H., Zhao, J., Shen, J. W., Sun, H. T., et al. (2021). Study on fracturing fluid adaptability in unconventional multi-target reservoir. *Petrochem. Indus Appl.* 40, 72–75.

Li, P., Ma, D. M., Zhang, H., Li, W. B., and Yang, F. (2016). Influence of high and low rank coal wettability and methane adsorption/desorption characteristics. *Coal Geo. Explor.* 44, 80–85.

Li, P., Zhang, X., Li, J., Zhao, J., Huang, J., Zhang, S., et al. (2020). Analysis of the key factors affecting the productivity of coalbed methane wells: A case study of a high-rank coal reservoir in the central and southern Qinshui Basin, China. *ACS omega* 5, 28012–28026. doi:10.1021/acsomega.0c03540

Li, X., Zhang, J., Li, R., Qi, Q., Zheng, Y., Li, C., et al. (2021). Numerical simulation research on improvement effect of ultrasonic waves on seepage characteristics of coalbed methane reservoir. *Energies* 14, 4605. doi:10.3390/en14154605

Liu, S., and Harpalani, S. (2013). Permeability prediction of coalbed methane reservoirs during primary depletion. *Int. J. Coal Geol.* 113, 1–10. doi:10.1016/j.coal.2013.03.010

Liu, S. T., Zheng, Z. H., Geng, M., Jiao, J., Gao, Y., and Wu, J. P. (2019). Resources potential and exploration prospect of coalbed methane in Qinshui basin. *China Min. Mag.* 28, 37–43.

Lu, Y., Shelepov, V. V., Yang, Z., Liu, J., Han, J., Guo, J., et al. (2018). Research on initial pressure of fracture in the technique of staged fracturing of a horizontal well. *J. Appl. Mech. Tech. Phy.* 59, 1111–1117. doi:10.1134/s0021894418060172

Min, C., Zhang, X. H., Yang, Z. Z., Li, X. G., and Dai, B. R. (2022). Identification of main controlling factors of fracturing performance in coalbed methane wells based on CBFS-CV algorithm. *Pet. Geol. Rec. Eff.* 29, 168–174.

Salmachi, A., Rajabi, M., Wainman, C., Mackie, S., McCabe, P., Camac, B., et al. (2021). History, geology, *in situ* stress pattern, gas content and permeability of coal seam gas basins in Australia: A review. *Energies* 14, 2651. doi:10.3390/en14092651

Teufel, L. W., and Clark, J. A. (1984). Hydraulic fracture propagation in layered rock: Experimental studies of fracture containment. *Soc. Petroleum Eng. J.* 24, 19–32. doi:10.2118/9878-pa

Wang, S., Zhang, Y., Guo, J., Lai, J., Wang, D., He, L., et al. (2014). A study of relation between suspension behavior and microstructure and viscoelastic property

of guar gum fracturing fluid. *J. Pet. Sci. Eng.* 124, 432–435. doi:10.1016/j.petrol.2014.09.016

Xu, T., Mao, J., Zhang, Q., Lin, C., Yang, X., Zhang, Y., et al. (2021). Synergistic polymer fracturing fluid for coal seam fracturing. *Colloids Surfaces A Physicochem. Eng. Aspects* 631, 127648. doi:10.1016/j.colsurfa.2021.127648

Xue, H. F., Zhu, G. H., Wang, W., Lu, X. X., Wang, M. H., and Wang, Y. B. (2019). Analysis and application of key influencing factors of CBM well fracturing effects in Shizhuang area, Qinshui basin. *Coal Geol. Explor.* 47, 76–81.

Yu, Y. J., Zhu, W. C., Li, L. C., Wei, C. H., Zhang, X. F., Qin, C., et al. (2019). Simulations on hydraulic fracture propagation of coal-rock combination in deep underground. *Hazard Control Tunn. Und. Eng.* 1, 96–108.

Zhang, X. Y. (2018). "Optimization model of quantitative drainage system for CBM vertical wells in Zhengzhuang block," ([Xuzhou (Jiangsu)]: China University of Mining and Technology) ([Dissertation/doctoral thesis].

Zhang, Z., Wang, H., Deng, B., Li, M., and Zhang, D. (2018). Field investigation of hydraulic fracturing in coal seams and its enhancement for methane extraction in the Southeast Sichuan Basin, China. *Energies* 11, 3451. doi:10.3390/en11123451

Zhu, Q. Z., Zhang, X. D., Yang, Y. H., Hu, X. F., Zhang, Y. P., Yang, Y. L., et al. (2018). Geological factors affecting desorption pressure of CBM wells in the southern and central-southern Qinshui Basin and their influencing mechanism. *J. China Univ. Pet.* 42, 41–49.